Lab on a Chip

Accepted Manuscript

ROYAL SOCIETY OF CHEMISTRY

www.rsc.org/loc

Lab on a Chip

RSCPublishing

TECHNICAL INNOVATION

A novel MEMS compatible lab-on-a-tube technology

Cite this: DOI: 10.1039/xoxxoooooox

Zhuoqing Yang, Yi Zhang *, Toshihiro Itoh and Ryutaro Maeda

Received ooth January 2012,
Accepted ooth January 2012

DOI: 10.1039/xoxxoooooox

www.rsc.org/

We present a novel lab-on-a-tube technology, which is a combination of three-dimensional (3D) cylindrical photolithography and nanoimprint process, for fabricating micro functional structures on tiny tube substrate directly. As example, electrochemical electrodes, which consisted of Pt work and Ag/AgCl reference electrode, were successfully fabricated on a 330 μm-diameter polyimide capillary. Using thermal nanoimprint technology, micro dome array with the diameter from 2 μm down to about 600 nm were prepared in the work and reference electrode. The nanoimprint domes greatly enhanced the electrochemical activity and there were much higher oxidation and reduction current peak observed in cyclic voltammetry curves of the nanoimprint electrode than the blank electrode without the nanoimprint modification. The nanoimprint patterns exhibited complicated effects, e.g. the 600 nm-diameter dome sample had higher electrochemical activity than the 2 μm-diameter one, while the latter had larger surface. By using the new lab-on-a-tube technology, new bio and nanomaterials could be integrated directly into electronic devices on tiny tube substrates so that many interesting applications could be expected in medical and life technologies.

1. Introduction

With the rapid progress of bio and life technology, micro sensors are required in monitoring application of chemical and bio reactions in tiny objects or small volumes such as cell and blood vessels.[1] Therefore, smart tube [2], lab on a tube [3] and other similar technologies [4] are under developing in order to fabricate micro sensors and other functional structures directly onto tiny and flexible tube, capillary and fibre substrates.[5] Li et al [3] prepared various sensors on ribbon substrate, and then stacked, bonded and rolled it spirally on a cylindrical support to form a smart tube. By using this method, micro sensors can be placed on the inside and outside of the smart tube, which allows for monitoring of the global and the local information.[3, 6] Many researchers are also working on the development of smart catheters and tube systems by using lithography, transfer printing and other technologies.[4-5, 7-10] For example, balloon catheters are successfully fabricated as an solution to the challenge in establishing biocompatible interfaces between the classes of semiconductor device and sensors, and the soft, curvilinear surface of living tissue.[7] Very recently, Xu et al [4] developed a post silicon-on-insulator compatible parylene smart tube technology, in which conventional CMOS and MEMS processes are utilized for preparing circuits and sensors.

As a matter of facts, most of the aforementioned methods are still mainly involved of planar processes so that tube-like devices are realized through complicated integrating or even spirally rolling on a tube substrate. As a result, there are still many efforts on fabricating micro sensors on tube-like substrates directly. Laser-lathe technology [9] is under developing for directly preparing coil structure and even more complicated functional structures on tiny capillary. Haga et al.[10] have been working on smart catheters through directly fabricating micro sensors on tiny capillary by using laser lithography method. These two laser-based technologies are either involved of special resist materials or have limited resolution, so that they are difficult to be utilized for integrating those new bio and nanomaterials with semiconductor devices and sensors on tiny tubes directly.

Very recently, we have suggested a 3D cylindrical projection photolithography method for directly fabricating micro coil and micro temperature sensors on tiny capillary, which has the diameter of from 1 mm down to 300 μm.[11-12] The prepared micro temperature sensor on 330 μm-diameter capillary exhibited excellent performance because of little hysteresis effect of the substrate.[12] The minimum feature size has been successfully reduced to about 10 μm by using the 3D cylindrical projection photolithography method. The new 3D cylindrical projection photolithography method is mainly involved of conventional photolithography material and process, so that it would be a good solution to the challenge in direct integration of semiconductor device and sensor onto tiny tube and fabric substrates. In addition, comparing with its laser technology-based counterparts,[9-10] the new 3D cylindrical photolithography technology has much shorter process time and thus higher throughput because not only programmable stages and enhanced software are used but also a mask supported by a programmable stage is utilized for assisting the exposure process. Therefore, we thought that more interesting applications could be further expected if the new 3D cylindrical photolithography process could be combined with others for integrating those bio and nanomaterials, which are generally polymers, onto tube substrate directly.

Research Center for Ubiquitous MEMS and Micro Engineering, National Institute of Advanced Industrial Science and Technology (AIST), Tsukuba, Japan. Email: yi.zhang@aist.go.jp

Nanoimprint technology is considered to be one solution to the integration issue of the bio and nanomaterials with conventional electronic devices.[13] It can not only be used to form patterns in polymers, but can also be extended to create functional polymer structures directly. In addition, different from conventional photolithography technology, the nanoimprint technology relies on direct mechanical deformation even at room temperature, so that it has many potential applications in energy, bio and medical technology.[13-14] therefore, in this work, we would present a new micro-electro-mechanical system (MEMS) lab-on-a-tube technology by combining the nanoimprint process with the 3D cylindrical projection photolithography technology, and fabricate micro electrochemical electrode on tiny capillary as example also because it is among the most commonly used devices in bio and life science.

2. Experimental

Figure 1 shows sketch of micro electrochemistry electrode on a 330 μm-diameter polyimide capillary, which would be fabricated in this work. Nanoimprint structure is directly fabricated on the polyimide capillary. It is well known that the nanoimprint of polyimide polymer is difficult. [15] However, because of its excellent thermal and chemical stability, the polyimide capillary is utilized as

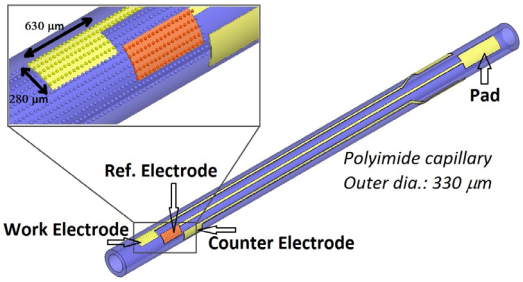

Fig. 1 Sketch of electrochemical electrode on a polyimide capillary with the outer diameter of 330 μm and the inner diameter of 250 μm.

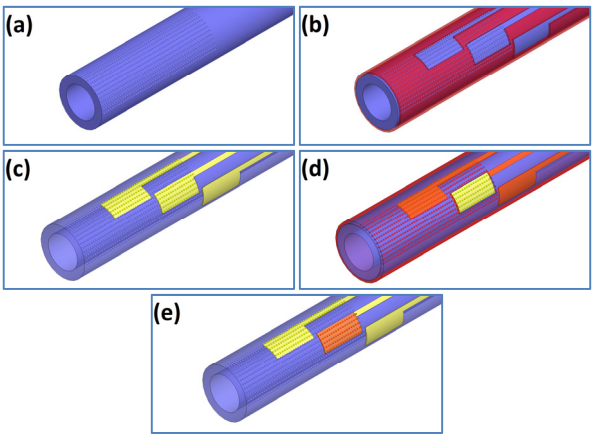

Fig. 2 Fabrication sequence of the electrochemical electrode. (a) Nanoimprint of polyimide capillary; (b) Photoresist deposition and 3D cylindrical photolithography; (c) Deposition and lift-off of thin Pt/Ti film; (d) Photoresist deposition and 3D cylindrical photolithography; and (e) Deposition and modification of Ag film. The lift-off of the Ag/AgCl film was performed and only one electrode was coated with the Ag/AgCl film for forming the reference electrode.

the substrate. The micro electrode is 630 μm long and 280 μm wide. The work and counter electrode are made of Pt film with the thickness of about 100 nm. The reference electrode is made of Ag/AgCl film. The work and reference electrode are prepared in the nanoimprint area.

Figure 2 shows fabrication sequence of the electrochemical electrode sample. The polyimide capillary has an inner diameter of 250 μm. Micro dome patterns were prepared on the polyimide capillary directly by using a planar silicon-based nanoimprint mould, in which there are holes array. Two kinds of holes pattern including the diameter/pitch/depth of 0.5 μm/1.5 μm/1 μm, and 2 μm/4 μm/2 μm, respectively, were utilized. The nanoimprint process was carried out in a thermal nanoimprint system (NI213, Nano Craft Tech., Japan) under the optimized conditions of 400°C and pressure of 30 MPa. Stainless wire with the diameter of 250 μm was inserted into the polyimide capillary as a solid support; otherwise the capillary would collapse much during the nanoimprint. The nanoimprint pattern was only formed on one side of the capillary substrate. The de-moulding temperature was 60°C. Thin film of resist was coated on the substrate and then exposed in the cylindrical projection photolithography system (see Fig. 2 (b)). The cylindrical projection photolithography system was introduced in details in our previous report.[12] Thin Pt film was deposited by using sputtering method and patterned by ultrasonically rinsing in alcohol solution in order to remove underneath resist layer. During the sputtering, the capillary substrates were rotated by using a home-made fixture, in which four capillary substrates can be loaded at one time, for achieving thin and uniform films of Pt. The samples were rinsed with purified water, dried, and then coated with thin resist film again. After the second time alignment and exposure, 500 nm-thick Ag film was deposited by using sputtering method and modified into AgCl by immersing into a 0.4 mol/L KCl solution for two hours. In order to achieve same surface conditions, several capillary samples were treated together. Finally, the sample was rinsed in acetone for removing the residual resist. The Ag/AgCl film was only remained in the reference electrode. The nanoimprint patterns were examined by using scanning electron microscope (SEM) and atomic force microscopy (AFM) (SPI3800, Seiko Instruments Inc., Japan). Cyclic voltammetry test was performed to examine the basic properties of the prepared micro electrodes and the effect of the nanoimprint patterns as well. The cyclic voltammetry experiments were carried out in a solution of 1 mol/L KCl containing 0.02 mol/L $K_3Fe(CN)_6$ at the room temperature by using an electrochemical analyser (ALS/CHI 600E, CHI Instruments Inc, USA). Due to the difficulty of wiring, the prepared devices were characterized in the configuration of two-electrode. Although the electrochemical measurement of two-electrode configuration is less accurate than the three-electrode counterpart, the distance between the reference and work electrode is very short in the prepared samples so that the measurement is still acceptable.

3. Results and discussion

Figure 3 shows SEM and AFM image of the Pt-coated nanoimprint patterns on the polyimide capillary. AFM measurement indicated that by using the holes pattern of the diameter/pitch/depth of 0.5 μm/1.5 μm/1 μm, the as-prepared micro dome array had the diameter/pitch/height of 0.6 μm/1.5 μm/0.2 μm. By using the holes pattern of 2 μm/4 μm/2 μm, the achieved micro dome array has the diameter/pitch/height of 2 μm/4 μm/0.6 μm. It indicated that the prepared micro domes have lower height than expected. It was mainly related to that the nanoimprint process was not performed in vacuum. There were strong resistances resulted from the enclosed air in the micro hole pattern of the nanoimprint mould. It was also

found that the 600 nm-diameter micro dome had the irregular morphology while the 2 μm-diameter ones were of typical dome shape. These irregular shape of the 600 nm-diameter micro dome was mainly resulted from the deformation occurred during the de-moulding process. The surface enlargement resulted from the 600 nm and 2 μm-diameter micro domes were about 12% and 20%, respectively. Figure 4 shows SEM image of the nanoimprint patterns after the sputtering of Ag film. The 600 nm-diameter patterns became smaller and more irregular, because the Ag film was about 500 nm thick. Helix growth morphology of Ag film is visible. The 2 μm-diameter patterns still remain their original shapes and there is visible polycrystalline morphology of Ag film. SEM observations also showed that the surface enlargement of the 600 nm-diameter dome pattern was reduced after the deposition of Ag film because it has limited height.

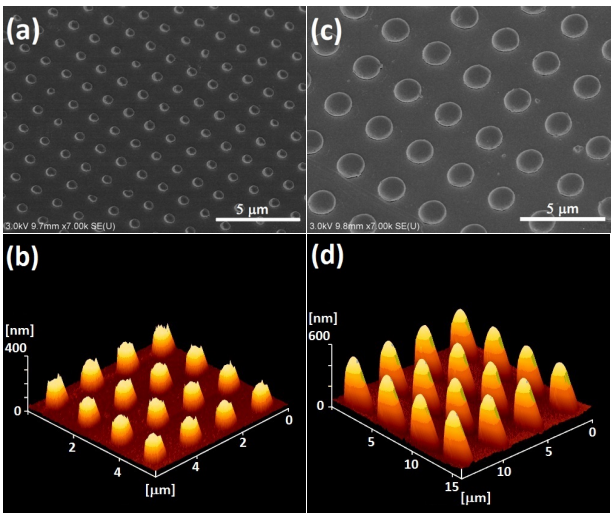

Fig. 3 SEM photography and AFM images of the nanoimprint patterns on the 330 μm-diameter polyimide capillary. There was a 100 nm-thick Pt film deposited. (**a** & **b**) the 600 nm-diameter micro dome; (**c** & **d**) the 2 μm-diameter micro dome.

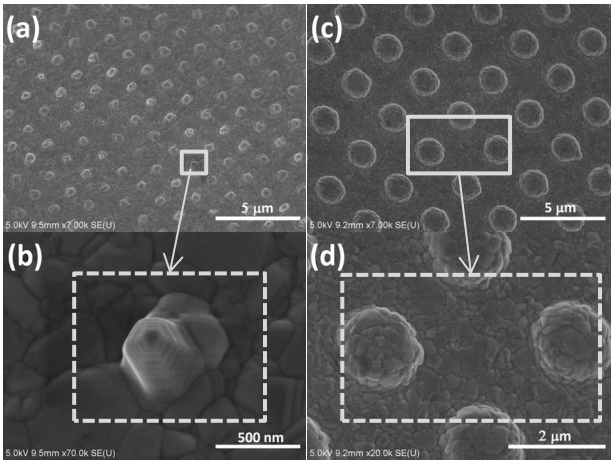

Fig. 4 SEM photography of the nanoimprint patterns after the deposition of the 500 nm-thick Ag film. (**a** & **b**) the 600 nm-diameter micro dome; (**c** & **d**) the 2 μm-diameter micro dome.

Figure 5 shows SEM photography of the fabricated micro electrochemistry electrode on the 330 μm-diameter polyimide capillary. Work and reference electrodes were located in the nanoimprint area. Figure 6 shows measured cyclic voltammetry (CV) plots of the prepared electrodes in the solution of 1 mol/L KCl containing 0.02 mol/L $K_3Fe(CN)_6$ without the stir at room temperature. The scan rate was 10 mV/second. For direct comparisons, micro electrode sample without the nanoimprint modification, i.e. the blank electrode, was also fabricated and characterized. There are not obvious redox peaks in the CV plot of the blank electrode. It also indicated the electrochemical

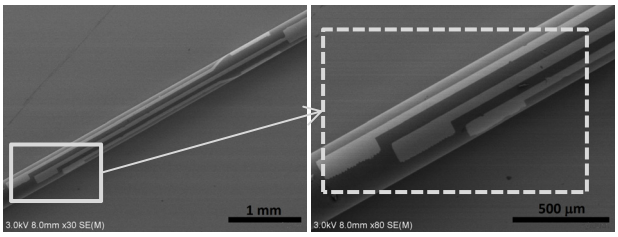

Fig. 5 SEM photography of the prepared micro electrochemical electrode on the 330 μm-diameter polyimide capillary.

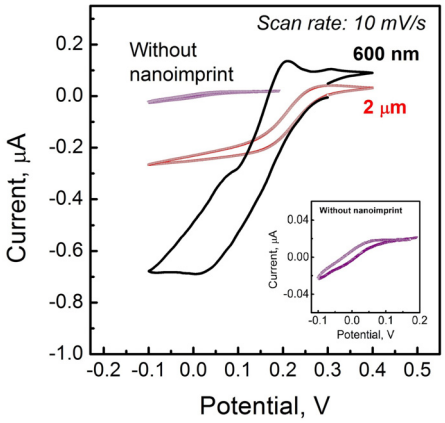

Fig. 6 Measured cyclic voltammetry plots of the prepared samples including the blank sample without the nanoimprint modification (also see enlarged insert). The electrode area is about 630 μm long and 280 μm wide.

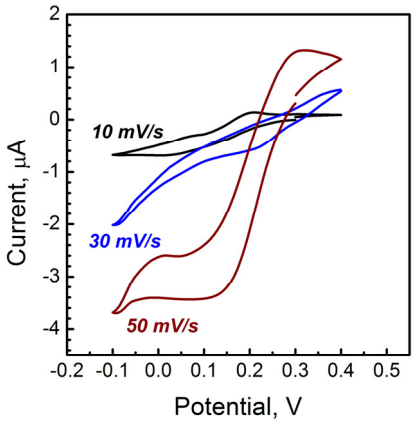

Fig. 7 Measured scan-rate dependency of cyclic voltammetry plots of the micro electrochemical electrode with the nanoimprint pattern of the 600 nm diameter. The electrode area is about 630 μm long and 280 μm wide.

reaction of the blank electrode was irreversible. Similar phenomenon had been encountered in the CV characterization of those electrochemical electrodes prepared by using microfabrication mehtod.[16] As a result, there are numerous efforts on developing modification technology of the microfabricated electrochemical electrodes, e.g. by using C-MEMS method,[14, 17] porous material and structure, [18] and 3D structures. [19-20] Figure 6 demonstrated that with the presence of the nanoimprint structure, the measured CV plots have larger redox currents than that of the blank sample, suggesting that the nanoimprint pattern had obviously increased the electrochemical activity. It indicated that the nanoimprint technology could be one good solution for enhancing activity of tiny electrochemical electrode also because of its advantage of simple and easy-to-control process.

In addition, Fig. 6 shows that the electrochemical electrode with the 600 nm-diameter dome pattern exhibited larger redox currents than that with the 2 μm-diameter dome pattern. As a matter of facts, the surface enlargement due to the 600 nm-diameter dome was about 12%, which is smaller than that of the 2 μm-diameter dome pattern, i.e., about 20%. In particular, with the coating of the 500 nm-thick Ag film, the dome height decreased much from its original 200 nm height. SEM observation showed that the 600 nm-diameter micro dome became into small tips after the coverage of Ag film. It could be thus inferred that the increase of the electrochemical activity is not only related to the active area but also other factors. In Fig. 6, another worthy to note is that there are broad bands in of the CV plot of the 600 nm-diameter sample. Such a phenomenon of the broad band often results from the charging effect of micro crack and other similar defects of electrode during electrochemical reaction.[16] Because of different thermal expansion coefficient of metal film and the polyimide material, there might be some micro cracks occurred in the prepared electrochemistry electrodes. As a matter of facts, there are few micro cracks morphologies visible in the prepared electrochemistry electrodes including the nanoimprint and blanks one. It suggested that there are other factors except for micro cracks responsible for the broad band phenomenon of the measured CV plots.

Fig 7 shows that scan-rate dependence of the CV plots of the 600 nm-diameter dome electrochemical electrode. There was strong dependence of scan rate. With the increase of the scan rate, the current of redox current became much larger, suggesting that the electrochemical system is basically diffusive. Another point worthy to note is that although both the reduction and oxidation peak current changed much with the increase of the scan rate, the former had larger variation than the latter in the CV plots of the nanoimprint electrode. Such a shift of the CV plot to either anodic or catholic side is often related to the phenomenon of electron mediation occurred on the electrode. In addition, the shape of the CV plots changed with the scan rate, indicating that there are additional reactions occurred on the nanoimprint electrode. The reason and mechanisms are unclear but it might be related to the nanoimprint patterns. Very recently, it has been found that nano particle and structure strongly modify electrode and thus change electrochemical performances.[19-21] For example, these nano particle and structure not only result into either higher redox currents, but also morphology-dependent electrochemical reactions. Although the nanoimprint dome has the diameter of about 600 nm, its height is only 200 nm and reduces much after the deposition of the 500 nm-thick Ag film. It might result into the formation of some nanostructures and complicated electrochemistry reactions.

4. Conclusions

Micro electrochemical electrodes with high activity are successfully prepared on tiny polymer capillary directly by using a combined method of the nanoimprint and the 3D cylindrical photolithography process. The nanoimprint electrodes exhibited interesting potential in bio and medical applications because it could be integrated with new functional materials directly. However, it was also found that the nanoimprint patterns have complicated effects on the electrochemical reaction. For example, the CV measurements indicated that the nanoimprint patterns not only enhanced the electrochemical activity, but also increased the catalyst effect of the electrode materials, which mainly consisted of thin sputtered films. The latter effect was responsible for the occurrence of electron mediation-like phenomenon shown in the measured CV plots. Therefore, more effort is still needed for understanding the effect of nanoimprint pattern. Considering the advantages of the nanoimprint such as easy-to-control, simple, low cost and etc., the new MEMS compatible lab-on-a-tube technology of this work could be expected for more interesting applications after the complicated effects of the nanoimprint pattern are clarified.

References

1 B. Tian, J. Liu, T. Dvir, L. Jin, J. H. Tsui, Q. Qing, Z. Suo, R. Langer, D. S. Kohane, C. M. Lieber, *Nat. Mat.*, 2012, 11, 986-994.
2 C. Li, P. Wu, J. A. Hartings, Z. Wu, C. H. Ann, D. LeDoux, L. A. Shutter, R. K. Narayan, *Appl. Phys. Lett.*, 2011, 99, 233705.
3 C. Li, P. Wu, W. Jung, C. H. Ann, L. A. Shutter, R. K. Narayan, *Lab Chip*, 2009, 9, 1988-1990.
4 H. Tu, Y. Xu, *Lab Chip*, 2013, 13, 1027-1030.
5 M. Focke, D. Kosse, C. Muller, H. Reinecke, R. Zengerle, F. Stetten, *Lab Chip*, 2010, 10, 1365-1386.
6 J. Williams, *Lab Chip*, 2009, 9, 1987.
7 D. Kim, N. Lu, R. Ghaffari, Y. Kim, S. P. Lee, L. Xu, J. Wu, R. Kim, J. Song, Z. Liu, J. Viventi, B. Graff, B. Elolampi, M. Mansour, M. J. Slepian, S. Hwang, J. D. Moss, S. Won, Y. Huang, B. Litt, A. Rogers, *Nat. Mater.*, 2011, 10, 316-323.
8 Y. Li, H. Tu, R. Iezzi, P. Finlayson, Y. Xu, *J. Micromech. Microeng.* , 2011, 21, 115005.
9 V. Demas, A. Bernhardt, V. Malba, K. L. Adams, L. Kvans, C. Harvey, R. S. Maxwell, J. L. Herberg, *J. Magn. Reson.*, 2009, 200, 56-63.
10 Y. Haga, T. Matsunaga, W. Makishi, K. Totsu, T. Mineta, M. Esashi, *Minimally Invasive Therapy*, 2006, 15:4, 218-225.
11 S. Uchiyama, Z. Yang, A. Toda, M. Hayase, T. Itoh, R. Maeda, Y. Zhang, *J. Miromech. Microeng.*, 2013, 23, 114009.
12 Z. Yang, Y. Zhang, T. Itoh, R. Maeda, *J. Microelectromech. Sys.*, 2014, 23, 21-29.
13 L. Guo, *Adv. Mater.*, 2007, 19, 495-513
14 Y. Qiu, Y. Zhao, X. Yang, W. Li, Z. Wei, J. Xiao, S. Leung, Q. Lin, H. Wu, Y. Zhang, Z. Fan, S. Yang, *Nanoscale*, 2014, 6, 3626-3631.
15 S. Siqing, H. Wu, A. Takahara, *Polymer J.* 2012, 44, 1036-1041.
16 M. Beidaghi, W. Chen, C. Wang, *J. Power Source.*, 2011, 196, 2403-2409.
17 M. Beidaghi, C. Wang, *Electrochimica Acta*, 2011, 9508-9514.
18 L. Oakes, A. Westover, J. W. Mares, S. Chatterjee, W. R. Erwin, R. Bardhan, S. M. Weiss, C. L. Pint, *Scientific Reports*, 2013, 3: 3020
19 X. Liu, H. Jung, S. Kim, H. Choi, S. Lee, J. Moon, J. Lee, *Scientific Reports*, 2013, 3: 3183.
20 Y. Qiu, Y. Zhao, X. Yang, W. Li, Z. Wer, J. Xiao, S. Leung, Q. Lin, H. Wu, Y. Zhang, Z. Fan, S. Yang, *Nanoscale*, 2014, 6, 3626-3631.
21 S. R. Belding, R. G. Compton, *J. Phys. Chem. C*, 2010, 114, 8309-8319.

